

Reparation and properties of porous ceramics via re-coating technique

Zhou Mei, Dai Wubin* and Zeng Lingke

School of Materials Science and Engineering, South China University of Technology, Guangzhou, Guangdong, 510640, P. R. China

Via a polymeric foam replication and two-step route (heating and re-coating), the reticulate porous ceramics (RPCs) were fabricated. The coating slurries were made up mainly by the ceramic powder (major raw material) and silica sol (binder). The re-coating slurries were obtained by mixing the pore-forming raw material with dilute coating slurries. The effect of the solid-contents on the re-coating rate (P_r) and the porosity (θ_p) was investigated. The experimental results indicate that the P_r is increasing and the θ_p is decreasing gradually following the increase of solid-contents. The specific surface area and the pore size distribution of the sintered bodies were measured by intrusive mercury curve. Morphological characteristics of the sintered bodies were investigated by the scanning electron microscopy (SEM). The results illustrated that the pore diameter were all quite spread and the effective specific surface areas for the samples G-4, S-4 and D-4 RPCs are 0.36 m²/g, 0.52 m²/g and 1.63 m²/g, respectively.

Key words: Reticulate porous ceramic, Re-coating technique, Pore-forming materials, Effective specific surface area.

Introduction

The replication process (i.e., the polymeric sponge process) has become the most popular method [1, 2] which is always adopted to produce the reticulate porous ceramics (RPCs). Typically, the so-called cellular-structured RPCs composed of three-dimensional interconnected pores network are known by their high-performance properties, namely, high porosity, high strength, acid and alkali resistant [3-6]. These highly porosity materials have been using in a variety of fields, such as the filters for molten metal, hot gas and diesel engine exhausts, catalyst and carriers, biomaterials, thermal insulators for furnaces and aerospace applications, gas combustion burners and lightweight building materials and et al [7-14]. Because the RPCs have the properties of the remarkable high specific surface area, good penetrability, high mass transfer and low-pressure drop [15-17], this kind of materials had been also widely used for immobilizing microalgae and *saccharomyces cerevisiae* [18, 19]. Although RPCs can be also used as the organism carrier, they need have high effective specific surface area [20, 21].

The pore size of the RPCs can be examined and calculated by the result of intrusive mercury curve. The effective specific surface area is only associated to the surface area (ignoring the effect of the pores size below 10 microns from surface). In this work, the RPCs with large effective specific surface area are fabricated through the polymeric foam replication process within

two-step route (pre-sintering and re-coating). Actually, Ravault Frank [22] and Zhu Xin-Wen [23] were adopted this method to enhance the strength of the RPCs a long time ago. In this study, we concentrate our efforts on improving the specific surface area which is quite different when compared to the works before.

Experimental section

Raw materials

Commercial polyurethane foams (PU) with pore size 13 ppi (50 mm × 50 mm × 25 mm, Luoyang Jinling Mesh foam Factory, PRC) were chosen as the plate. The industrial ceramic powders with mean particle size at ~ 11.46 μm (Foshan Oceano Ceramic Co., Ltd., PRC) were used as the major raw materials. The commercial silica sol (with composition as SiO₂-21wt%, Na₂O-0.3wt%, PH = 8.5 ~ 10, Shanghai Changquan Silica Gel desiccant Co., Ltd., PRC) was employed as the binder. The slurry mixtures (used for coating) were prepared by mixing with distilled water (the detail components were shown in Table 1).

During the process of re-coating, the soluble starch (Shanghai Aibi Chemistry Preparation Co., Ltd. PRC), graphite (Qingdao Tianhe Graphite Co., Ltd. PRC) and diatomite (Shanghai Aibi Chemistry Preparation Co., Ltd. PRC) were added into low concentration slurry to make the starch, graphite and diatomite re-coating

Table 1. Components of the coating slurry.

Components	Ceramic powder	Distilled water	Silica sol
Mass percent (%)	65	34.55-35	0-0.45

*Corresponding author:
Tel : +86-20-87-11-42-17
Fax: +86-20-87-11-02-73
E-mail: wubin.dai@foxmail.com

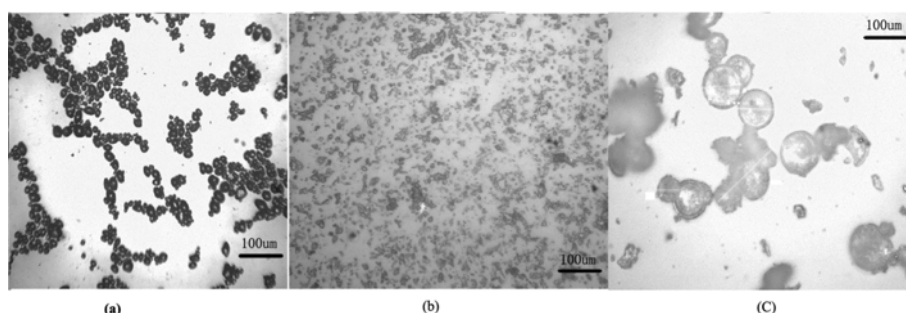


Fig. 1. Microscope images of the pore-forming material: (a) starch, (b) graphite, (c) diatomite.

Table 2. Components of the starch re-coating slurries samples.

Sample	Starch (wt%)	Ceramic powder (wt%)	Distilled water (wt%)
S-1	5	5	90
S-2	10	10	80
S-3	15	15	70
S-4	20	20	60
S-5	25	25	50

Table 3. Components of the graphite recoating slurries samples.

Sample	Graphite (wt%)	Ceramic powder (wt%)	Distilled water (wt%)
G-1	2	8	90
G-2	4	16	80
G-3	6	24	70
G-4	8	32	60
G-5	10	40	50

Table 4. Components of the diatomite recoating slurries samples.

Sample	Diatomite (wt%)	Ceramic powder (wt%)	Distilled water (wt%)
D-1	3.5	7	90
D-2	7	14	80
D-3	10.5	21	70
D-4	14	28	60
D-5	17.5	35	50
Y-1*	—	40	60

*the sample Y-1 means that there are no re-coating process.

slurries, respectively. The microscope images and particle sizes were shown in the Figure 1a to 1c. In order to explore the appropriate dosage, the amount of starch, graphite and diatomite has been studied in the present work when added as the solid-content for obtaining starch, graphite and diatomite re-coating slurries, respectively. The detailed components of a serial of starch re-coating slurries samples (ratio between starch and ceramic powder is keeping at the value of 1 : 1) are listed in Table 2. Similarly, for a serial of graphite re-coating slurries samples (the mass ratio between graphite and ceramic powder is fixed at 1 : 4), the content of each ingredient for the graphite re-coating slurries samples is exhibited in Table 3.

Meanwhile, for the diatomite re-coating slurries samples (the mass ratio between diatomite and ceramic powder is fixed at 1 : 2), the content of each ingredient for the diatomite re-coating slurries samples is exhibited in Table 4.

Experimental process

Firstly, the reticulated polymeric sponges were immersed into the coating slurries (see Table 1) and squeezed repeatedly to ensure that the slurries would be fulfilled all the void space. Secondly, the sponges passed through a set of rollers for removing the excess slurries. Thirdly, the as-coated sponges were dried and

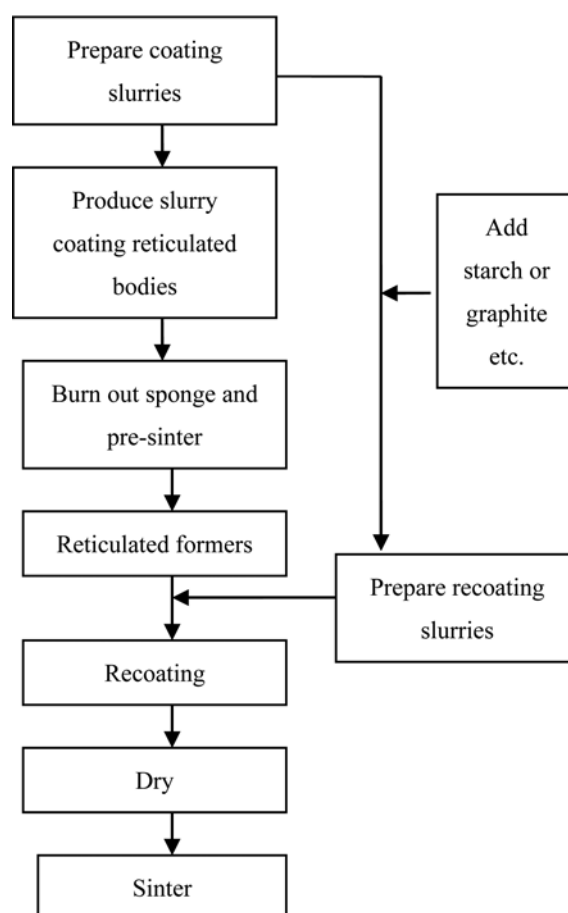


Fig. 2. Flow chart of the preparation of reticulate porous ceramics (RPC).

heated at temperature about 700 °C (the heating temperature was determined by the thermal gravity (TG) analysis). After these three steps, the sponges were burnt out and the reticulated formers with good strength for re-coating process were prepared. For the re-coating procedure, the reticulated formers were carefully dipped into the re-coating slurries (formula can be seen from Tables 2, 3 and 4) just for onesecond and then dried at 110 °C for 1 h. Next, the re-coated formers were sintered at 1150 °C to make the ultimate RPC samples. The reticulated formers before and after re-coating were weighed and their masses were represented by M_f and M_r , respectively. In order to clearly understand all this process, the whole experimental steps were sketched in Figure 2.

The amount of the starch, graphite and diatomite re-coating slurries on the reticulated formers can be described by the parameter of re-coating rate (P_r) which can be calculated by the formula (1):

$$P_r = \frac{M_r - M_f}{M_f} \times 100\% \quad (1)$$

Meanwhile, the porosity (θ_s) of the RPCs can be expressed by the formula (2):

$$\theta_s = \left(1 - \frac{\rho_b}{\rho_s}\right) \times 100\% \quad (2)$$

where ρ_b is the volume density of the RPC and ρ_s is the strut density, respectively. The pore size distributions of the sintered bodies were determined by the Pore Master 60 (Quanta chrome Corporation, USA). The effective specific surface area parameter S can be defined through the formula (3):

$$S = \frac{1}{\gamma \cos \theta} \int_{V_1}^{V_2} P dV \quad (3)$$

where γ is Hg Surface Tension and θ is Hg Contact Angle. Furthermore, the surface morphology of the sintered bodies was observed by SEM.

Results and Discussions

Typically, the re-coating rate is usually dominated by the viscosity of slurries, and this parameter is closely related to the kind of solids-content in the re-coating slurries (e.g., the starch, graphite and diatomite in this work). The effects of the solid-contents in the serial of the starch re-coating slurries on the parameters θ_s and P_r are shown in Figure 3. With increasing of the solid-contents starch in the coating slurries, the value of P_r is also increasing and oppositely, θ_s is dropping gradually. When the solid-contents increases from 10% to 50% as shown in Fig.3, accompanied by θ_s drops from 85% to 73%, P_r increases significantly from 0.2% to 19%. Most interesting and importantly, when the solid-contents reaches to 50%, the value of the parameters of P_r and θ_s changes much more obviously. Due to the

viscosity of the slurries increases incrementally and keeps good liquidity when the solid-contents increases from 10% to 40%, the slurries were coated uniformly on the pore surface in the reticulated formers. With increasing of the re-coating thickness, the P_r increases and θ_s decreases. However, when 50% of the solids-content in the re-coating slurries, the viscosity is abrupt became so high that the slurries cannot flow freely and block the pore in the reticulated performs during the re-coating process. Thus, it is safely to make a conclusion that the optimized solid-contents in the starch re-coating slurries is at ~40%.

In the same way, the effects of solid-contents in the samples (graphite and diatomite re-coating slurries) on the parameters θ_s and P_r were also investigated as shown in Figures 4 and 5, respectively. The results are found to be quite similar comparing to the case for starch re-coating slurries (shown in Fig. 3). Therefore, the amount of the solid-contents in the graphite and diatomite re-coating slurries are also optimized at the value ~40%.

The intrusive mercury curves for the RPC samples S-4, G-4 and D-4 are given in the supporting information (Figure S1 to S3). The effective specific surface areas of the samples Y-1, G-4, S-4 and D-4 RPCs are

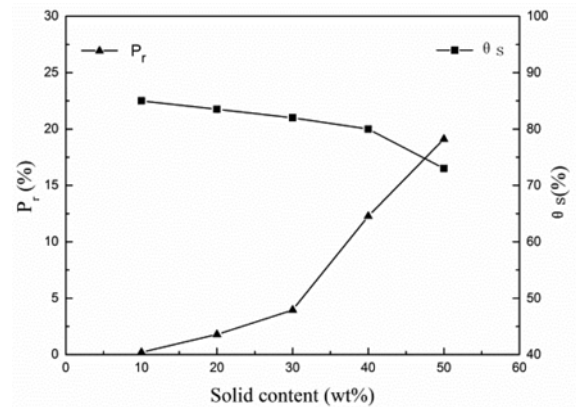


Figure.3 Effects of solids-content in the starch recoating slurries on θ_s and P_r .

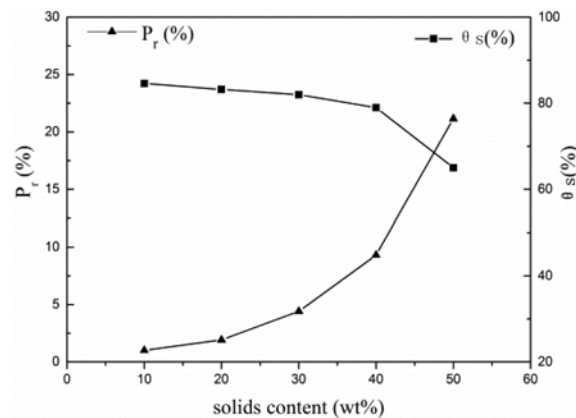


Fig. 4. Effects of solids-content in the graphite recoating slurries on θ_s and P_r .

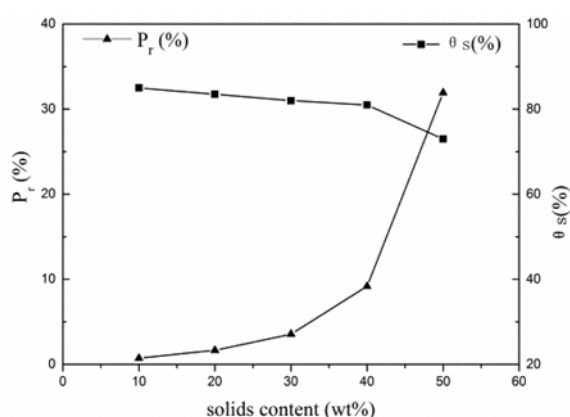


Fig. 5. Effects of solids-content in the diatomite recoating slurries on θ_s and P_r .

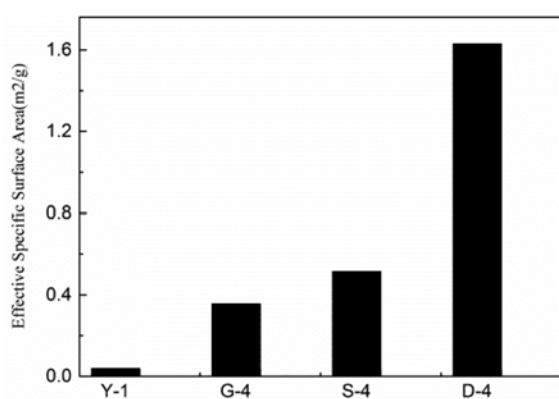


Fig. 6. Effective specific surface area of different RPC samples.

contrasted and the results are shown in Figure 6. From the result of the intrusive mercury curves, we can

conclude that the pore diameter is wide spread ranged from 200 μm to 500 μm for the RPC S-4, while the pore diameter for the G-4 RPC ranged from 500 μm to 1000 μm and the D-4 RPC ranged from 10 μm to 20 μm , respectively. The effective specific surface areas for the samples G-4, S-4 and D-4 RPCs are 0.36 m^2/g , 0.52 m^2/g and 1.63 m^2/g , respectively. Thus, the specific surface area for the sample S-4 RPC is 1.45 times higher than the sample G-4, the specific surface area for the sample D-4 RPC is more than 3 times higher than the sample S-4. Moreover, all the re-coated RPCs samples are more than ten times larger than the un-recoated RPC when compared the property of the specific surface area.

Actually, the formed pores after the re-coating process in the samples S-4 and G-4 RPCs are mainly due to the loss of the solid-contents starch and graphite (leaving vacancies in the framework structure) when sintered in high-temperature. However, for the D-4 RPC sample, after the processes of re-coating and sintering, the diatomite was peculiarly prone to adhere to the surface of the porous ceramic. Therefore, the main reason for the formed pores in the D-4 sample is because of the pores itself among the diatomite particles. The size of individual starch granule is between 10 to 30 μm (shown in Fig. 1a) while the final pore diameter of the S-4 sample is ranged from 200 to 500 μm (shown in Figure S1), which means that the agglomeration of starch granules occurs during the process of re-coating. According to the same reason, graphite particle is between 1 to 10 μm while pore diameter of the G-4 is ranged from 500 to 1000 μm (shown in Figure S2). As exhibited in Fig.1c, the

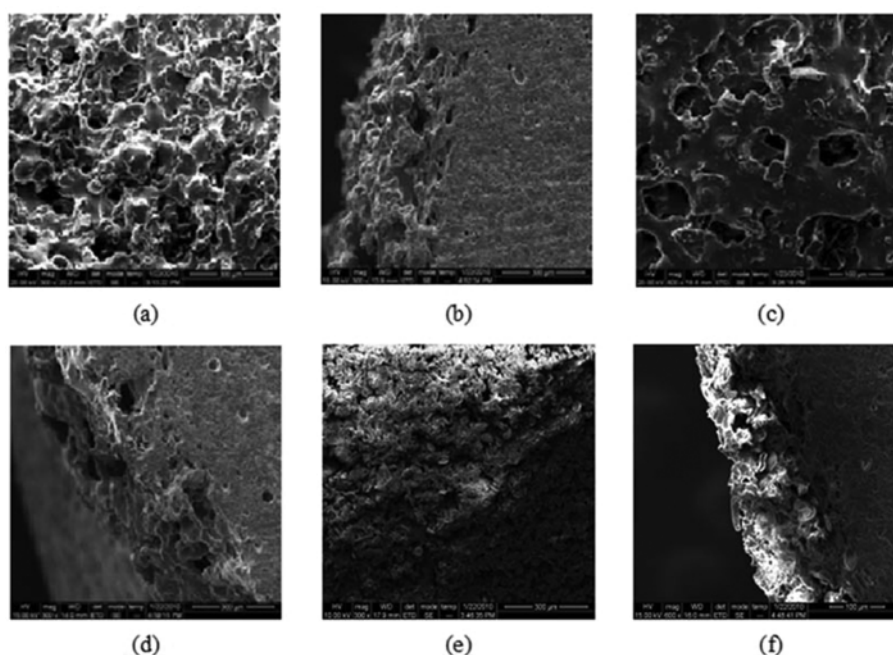


Fig. 7. SEM images of the surfaces and cross-sections in RPC samples: (a) surface of S-4, (b) cross-section of S-4, (c) surface of G-4, (d) cross-section of G-4, (e) surface of D-4, (f) cross-section of D-4.

particle diameter of the diatomite is normally around 40 μm , but the surface pore diameter of the D-4 sample is between 10 to 20 μm , which can confirm that the pore diameter is mainly due to the accumulation result of the diatomite particles.

The micro-structure of the surface and the cross-section images for the samples S-4, G-4 and D-4 RPCs are also exhibited in Figure 7a to 7f. As shown obviously in Figure 7a and 7c, there are plenty of pores on the surface for both the S-4 and G-4 samples. Relatively, the pores texture of the sample S-4 is more intricate and rugged than the sample G-4 because its pores size ranging from ten to thousand micron (more wide spread) and those pores with various size mixed together randomly. These phenomena of the micro-structure characteristics indicated that the starch dispersed uniformly in the re-coated slurries while the graphite floated on the top of the slurries because of lighter weight and poor wettability during the preparation of the re-coating process. For the D-4 sample as shown in the Figure 7e, the diatomite particle was quite compacting and arranging on the surface. Meanwhile, from the Figure 7(b), 7(d) and 7(e), the images indicate that the coating of PRC combines well with the base, and there is no distinct layers can be seen from cross sections of the samples. All these micro-structure characteristics of the S-4, G-4 and D-4 samples were consistent well with the properties discussed above.

Conclusions

With increasing of solid-contents in the coating slurries for all three serials of samples, the value of the parameter P_r is increasing and oppositely, θ_s is decreasing gradually. It has proved that 40% of solid-contents in the coating slurries are the optimization value for starch, graphite and diatomite re-coating slurries. The samples S-4, G-4 and D-4 RPCs have much better properties after the process of sintering. Meanwhile, the sintered reticulate porous ceramic keeps highly-performance and large effective specific surface area. During the re-coating process, the property of dispersion is in the sequence: starch < graphite < diatomite. The specific surface area is all increasing because the different pore-making agent formed different pore diameter and led to different specific surface area. When using diatomite as the pore-making agent *via* the re-coating process for making the reticulate porous ceramics, the formed pores are in the surface of the D-4 sample because of the pores itself among the diatomite particles and the pore diameter is ranged from 10 to 20 μm . Differently, for the case of starch and graphite, the main reason for forming pores is due to the loss of the starch and graphite themselves when sintered in high-temperature. The pore diameter for S-4

and G-4 RPCs are wide spread and ranged from 200 to 500 μm and 500 to 1000 μm , respectively. The smaller the pore diameter, the greater the specific surface area. The specific surface area in the re-coated RPC increases more than ten times than the un-coated RPC.

Acknowledgments

This work is financially supported by the China Postdoctoral Science Foundation (Grant No: 2014M552019).

References

1. J. Saggio-Wojansky, C. E. Scott and W. P. Minnear, *Am. Ceram. Soc. Bull.* 71 [11] (1992) 1674-1682.
2. K. Schwartzalder, A. V. Somers, *Method of Making Porous Ceramic Articles*, Patent number: 3090094, U. S. 1963.
3. S. B. Bhaduri, *Adv. Performance Mater.* 24 [1] (1994) 205-211.
4. E. J. Williams and J. R. Evans, *J. Mater. Sci.* 31 [2] (1996) 559-603.
5. S.-r. Wang, H.-r. Geng, L.-h. Hui and Y.-z. Wang, *J. Mater. Eng. Perform.* 16 [1] (2007) 113-118.
6. J. Petrasch, F. Meier, H. Friess and A. Steinfeld, *Int. J. Heat Fluid Flow* 29 [1] (2008) 315-326.
7. S. Zuercher, K. Pabst and G. Schaub, *Appl. Catal., A: General*, 357 [1] (2009) 85-92.
8. Z. Taslicukur, C. Balaban and N. Kuskonmaz, *J. Eur. Ceram. Soc.* 27 [2-3] (2007) 637-640.
9. J. L  v  que, D. Rouzineau, M. Pr  vost and M. Meyer, *Chem. Eng. Sci.* 64 [11] (2009) 2607-2616.
10. E. C. Bucharsky, G. Schell and R. Oberacker, *J. Eur. Ceram. Soc.* 29 [10] (2009) 1955-1961.
11. Y. Zhang, X. Li, F. Feng, Y. Lin, Y. Liao, W. Tian and L. Liu, *Appl. Surf. Sci.* 255 [2] (2008) 409-411.
12. X. Miao, Y. Hu, J. Liu and A.P. Wong, *Mater. Lett.* 58 [3-4] (2004) 397-402.
13. Z. Song and B. Lin, *Min. Sci. Tech (China)* 20 [2] (2010) 248-253.
14. P. Colombo, *Key Eng. Mater.*, 206-213 (2002) 1913-1918.
15. Z. Wu, C. Caliot, F. Bai, G. Flamant, Z. Wang, J. Zhang and C. Tian, *Appl. Energ.* 87 [2] (2010) 504-513.
16. M. Ciarletta, B. Straughan and V. Tibullo, *Nonlinear Anal. Real.* 12 [5] (2011) 2839-2843.
17. F. C. Patcas, G. I. Garrido and B. Kraushaar-Czarnetzki, *Chem. Eng. Sci.* 62 [15] (2007) 3984-3990.
18. I. Moreno-Garrido, *Bioresour. Technol.* 99 [10] (2008) 3949-3964.
19. C. Jiangfeng, S. Zhongliang, L. Chengwei and Y. Qingguo, *Chn. Brw.* 204 [3] (2009) 109-111.
20. W. Yi, in "Development and Application of a Porous Carrier Used in Biofilm Reactors, in: Materials Science" (Xi'an University of Architecture and Technology Press, 2004) p. 24.
21. T. Weijun, in "Study on the Mechanism and Test of Biological Hardening Purification Directly for Polluted Streams, in: Materials Science" (Hohai University Press, 2005) p. 33.
22. F. Ravault and G. Ernest, *Production of Porous Ceramic Materials*, Patent number: 4004933, U. S. 1977.
23. J. D. Zhu, X. W. Tan, S. H. Zhang and Z. Quan, *J. Inorg. Mater.*, 17 [1] (2002) 79-85.